Passive Cooling of a Micromechanical Oscillator with a Resonant Electric Circuit

K. R. Brown,* J. Britton, R. J. Epstein, J. Chiaverini,† D. Leibfried, and D. J. Wineland

Time and Frequency Division, National Institute of Standards and Technology, 325 Broadway, Boulder, Colorado 80305, USA

(Received 8 May 2007; published 26 September 2007)

We cool the fundamental mode of a miniature cantilever by capacitively coupling it to a driven rf resonant circuit. Cooling results from the rf capacitive force, which is phase shifted relative to the cantilever motion. We demonstrate the technique by cooling a 7 kHz cantilever from room temperature to 45 K, obtaining reasonable agreement with a model for the cooling, damping, and frequency shift. Extending the method to higher frequencies in a cryogenic system could enable ground state cooling and may prove simpler than related optical experiments in a low temperature apparatus.

DOI: 10.1103/PhysRevLett.99.137205 PACS numbers: 85.85.+j, 05.40.Jc

Stimulated by the early work of Braginsky and collaborators [1,2], the quantum-limited measurement and control of mechanical oscillators continues to be a subject of great interest. If one can cool to the ground state of the oscillator, the generation of nonclassical states of motion also becomes feasible. For an atom bound in a harmonic well, laser cooling in a room-temperature apparatus can cool the modes of mechanical motion to a level with mean occupation numbers $\langle n \rangle < 0.1$ for oscillation frequencies $\sim$1–10 MHz [3,4]. This has made it possible to generate nonclassical mechanical oscillator states such as squeezed, Fock [5], multiparticle entangled [6], and (in principle) arbitrary superposition states [7].

For more macroscopic systems, smaller and smaller micromechanical resonators have approached the quantum limit through thermal contact with a cryogenic bath (for a summary, see [8]). Small mechanical resonators, having low-order mode frequencies of 10–1000 MHz, can come close to the quantum regime at low temperature ($<$1 K), and mean occupation numbers of approximately 25 have been achieved [9]. Cooling of macroscopic mechanical oscillators also has been achieved with optical forces. The requisite damping can be implemented by use of active external electronics to control the applied force [10–13] (see also [14]). Passive feedback cooling has been realized in which a mirror attached to a mechanical oscillator forms an optical cavity with another stationary mirror. For appropriate tuning of radiation incident on the cavity, a delay in the optical force on the oscillator as it moves gives cooling. This delay can result from a photothermal effect [15,16] or from the stored energy response time of the cavity [17–19]. Closely related passive cooling has been reported in [9,20].

We demonstrate a similar cooling mechanism where the damping force is the electric force between capacitor plates [21] that here contribute to a resonant rf circuit [2,22]. This approach has potential practical advantages over optical schemes: eliminating optical components simplifies fabrication and integration into a cryogenic system, and the rf circuit could be incorporated on-chip with the mechanical oscillator.

A conducting cantilever of mass density ρ is fixed at one end [Fig. 1(a)]. One face is placed a distance d from a rigidly mounted plate of area $w \times h$, forming a parallel-plate capacitor $C_c = \epsilon_0 wh/d$, where ϵ_0 is the vacuum dielectric constant. An inductor L_0 and capacitor C_0 in parallel with C_c form a resonant rf circuit with frequency $\Omega_0 = 1/\sqrt{L_0(C_0 + C_c)}$ and with losses represented by resistance R_0. We assume $Q_{\mathrm{rf}} \gg 1$, where $Q_{\mathrm{rf}} = \Omega_0 L_0/R_0 = \Omega_0/\gamma$ and γ is the damping rate.

We consider the lowest-order flexural mode of the cantilever, where the free end oscillates in the $\hat{x}$ direction [vertical in Fig. 1(a)] with angular frequency $\omega_c \ll \gamma$.

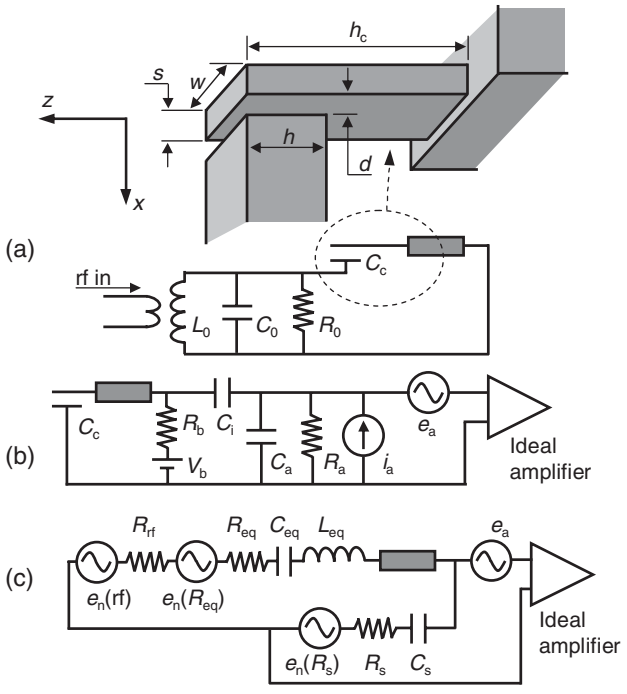

FIG. 1. Schematics of the cantilever cooling and detection electronics. (a) Cantilever and associated rf circuitry. (b) Motional detection electronics. Near ω_c the rf circuit looks like a short to ground as shown. (c) Equivalent circuit for the cantilever and detection electronics near $\omega \approx \omega_c$.

We take x to be the displacement at the end of the cantilever, so the displacement as a function of (horizontal) position z along the length of the cantilever is given by $x(z) = f(z)x$, where $f(z)$ is the mode function (see, e.g., [23]). Small displacements due to a force F can be described by the equation of motion,

$$m\ddot{x} + m\Gamma\dot{x} + m\omega_c^2 x = F, \tag{1}$$

where Γ is the cantilever damping rate and m its effective mass, given by $\rho\xi_c'' w h_c s$, where $\xi_c'' \equiv \frac{1}{h_c}\int_{h_c} f(z)^2 dz = 0.250$ for a rectangular beam.

For simplicity, first assume $h \ll h_c$, so that the force is concentrated at the end of the cantilever. If a potential V is applied across C_c, the capacitor plates experience a mutual attractive force $F = \epsilon_0 whV^2/(2d^2) = C_c V^2/(2d)$. Consider that V is an applied rf potential $V_{\rm rf}\cos(\Omega_{\rm rf} t)$ with $\Omega_{\rm rf} \approx \Omega_0$. Because $\omega_c \ll \Omega_0$, the force for frequencies near ω_c can be approximated by the time-averaged rf force

$$F_{\rm rf} = \frac{C_c\langle V^2\rangle}{2d} = \frac{C_c V_{\rm rf}^2}{4d} = \frac{\epsilon_0 whV_{\rm rf}^2}{4d^2}, \tag{2}$$

where, for a fixed input rf power, $V_{\rm rf}$ will depend on $\Delta\Omega \equiv \Omega_0 - \Omega_{\rm rf}$, according to

$$\frac{V_{\rm rf}^2}{V_{\rm max}^2} = \frac{1}{1 + [2Q_{\rm rf}\Delta\Omega/\Omega_0]^2} \equiv \mathcal{L}(\Delta\Omega). \tag{3}$$

As the cantilever oscillates, its motion modulates the capacitance of the rf circuit thereby modulating Ω_0. As Ω_0 is modulated relative to $\Omega_{\rm rf}$, so too is the rf potential across the capacitance, according to Eq. (3). The associated modulated force shifts the cantilever's resonant frequency. Because of the finite response time of the rf circuit, there is a phase lag in the force relative to the motion. For $\Delta\Omega > 0$ the phase lag leads to a force component that opposes the cantilever velocity, leading to damping. If this damping is achieved without adding too much force noise then it cools the cantilever.

The average force due to applied potentials displaces the equilibrium position d_0 of the cantilever. We assume this displacement is small and is absorbed into the definition of d_0, writing [24] $d \equiv d_0 - x$, where $x \ll d_0$. Following [2] or [22] we find $\omega_c^2 \to \omega_c^2(1-\kappa)$ and $\Gamma \to \Gamma + \Gamma'$, with

$$\kappa \equiv \frac{C_c V_{\rm max}^2 \mathcal{L}(\Delta\Omega)}{2m\omega_c^2 d_0^2}\left[\xi'' + \frac{2(\xi')^2 Q_{\rm rf}\Delta\Omega\,\mathcal{L}(\Delta\Omega)}{\gamma} \times \frac{C_c}{C_c + C_0}\right], \tag{4}$$

$$\Gamma' \equiv \frac{Q_{\rm rf} V_{\rm max}^2 C_c^2}{m\omega_c d_0^2 (C_c + C_0)}\frac{(\xi')^2\Delta\Omega\,\mathcal{L}(\Delta\Omega)^2}{\gamma}\sin\phi, \tag{5}$$

where $\xi' \equiv \frac{1}{h}\int_h f(z)dz$ and $\xi'' \equiv \frac{1}{h}\int_h f(z)^2 dz$ are geometrical factors required when $h \ll h_c$ is not satisfied. The phase ϕ is equal to $\omega_c\tau$, where $\tau = 4\mathcal{L}(\Delta\Omega)/\gamma$ is the response time of the rf circuit [25]. For $\Delta\Omega > 0$, Γ' gives increased damping. For $\Delta\Omega = \gamma/2$ and $h \ll h_c$ ($\xi' \approx \xi'' \approx 1$), we obtain the expressions of [22]. For our experiment, $h \approx h_c$, $\xi' = 0.392$, and $\xi'' = \xi_c'' = 0.250$.

We detect the cantilever's motion by biasing it with a static potential V_b through resistor R_b as shown in Fig. 1(b), where R_a, C_a, i_a, and e_a represent the equivalent input resistance, capacitance, current noise, and voltage noise, respectively, of the detection amplifier. We make R_a and R_b large to minimize their contribution to the current noise i_a. We assume $C_i \gg (C_c + C_a)$ and $\omega_c R(C_c + C_a) \gg 1$, where $1/R \equiv 1/R_b + 1/R_a$. As the cantilever moves, thereby changing C_c, it creates a varying potential that is detected by the amplifier.

The (charged) cantilever can be represented by the series electrical circuit in Fig. 1(c). From Eq. (2) and following [26], the equivalent inductance is given by $L_{\rm eq} = md_0^2/(q_c\xi')^2$, where q_c is the average charge on the cantilever. From $L_{\rm eq}$, ω_c, and Γ, we can then determine $C_{\rm eq} = 1/(\omega_c^2 L_{\rm eq})$ and $R_{\rm eq} = L_{\rm eq}\Gamma$. Additional damping due to the rf force is represented by $R_{\rm rf} = L_{\rm eq}\Gamma'$. For frequencies $\omega \approx \omega_c$, the parallel combination of R_b, C_a, and R_a can also be expressed instead as the Thévenin equivalent R_s-C_s circuit in Fig. 1(c). The amplifier's current noise i_a is now represented as $e_n(R_s)$. The intrinsic thermal noise of the cantilever is characterized by a noise voltage $e_n(R_{\rm eq})$ having spectral density $4k_B T_c R_{\rm eq}$, where k_B is Boltzmann's constant and T_c is the cantilever temperature.

We must also consider noise from the rf circuit. In Eq. (2), we replace $V_{\rm rf}$ with $V_{\rm rf} + v_n({\rm rf})$, where $v_n({\rm rf})$ is the noise across the cantilever capacitance C_c due to resistance in the rf circuit and noise injected from the rf source. The cantilever is affected by amplitude noise $v_n({\rm rf})$ at frequencies near $\Omega_{\rm rf} \pm \omega_c$, because cross terms in Eq. (2) give rise to random forces at the cantilever frequency. This force noise can be represented by $e_n({\rm rf})$ in the equivalent circuit. The noise terms sum to $e_n^2 = e_n^2(R_{\rm eq}) + e_n^2(R_s) + e_n^2({\rm rf})$ (e_a does not drive the cantilever), which gives a cantilever effective temperature

$$T_{\rm eff} = \frac{e_n^2}{4k_B(R_{\rm eq} + R_{\rm rf} + R_s)}. \tag{6}$$

Our cantilever has nominal dimensions $h_c \approx 1.5$ mm, $s \approx 14$ μm [27], and $w \approx 200$ μm, created by etching through a p^{++}-doped ($\sim$0.001 Ω cm), 200 μm thick silicon wafer with a standard Bosch reactive-ion-etching process. Its resonant frequency and quality factor are $\omega_c/(2\pi) \approx 7$ kHz and $Q \approx 20\,000$. The cantilever is separated by $d_0 \approx 16$ μm [27] from a nearby doped silicon rf electrode, forming capacitance C_c. The sample is enclosed in a vacuum chamber with pressure less than 10^{-5} Pa. The rf electrode is connected via a vacuum feedthrough to a quarter-wave resonant cavity with $L_0 = 330(30)$ nH and with loaded quality factor $Q_{\rm rf} = 234(8)$ at $\Omega_{\rm rf}/(2\pi) = 100$ MHz when impedance matched to the source. The cantilever is connected by a short length of coaxial cable and blocking capacitor $C_i = 4$ nF to a low-noise junction

field-effect transistor amplifier [see Fig. 1(b)]. We have $C_a = 48(1)$ pF, with $R_a = R_b = 1$ GΩ. We use $V_b = -50$ V, which gives a measured 2.5 μm static deflection at the cantilever end.

We temporarily lowered R_a to 600 kΩ $\approx 1/(\omega_c C_a)$, in which case the cantilever noise spectrum strongly distorts from a Lorentzian line shape (not shown), and it becomes straightforward to extract the equivalent circuit parameters of Fig. 1(c). We find $L_{eq} = 27\,000(600)$ H. To lowest order in rf power this equivalent inductance remains constant, so we assume this value for L_{eq} in subsequent fits to the thermal spectra, while R_{rf} is allowed to vary to account for rf power induced changes in the cantilever damping.

For $R_a = 1$ GΩ we measure $e_a = 1.5$ nV/$\sqrt{\text{Hz}}$ and $i_a = 16$ fA/$\sqrt{\text{Hz}}$. Figure 2 shows a series of thermal spectra acquired with this value of R_a at different values of rf power P_{rf} but at constant detuning $\Delta\Omega = 2\pi \times 90$ kHz $= 0.21\gamma$. Both the lowering and the broadening of the spectra with increasing P_{rf} are evident, in accordance with Eq. (5). Here, the effective temperature is very nearly proportional to the area under the curves, although there is a slight asymmetric distortion from a Lorentzian line shape, fully accounted for by the equivalent circuit model. The center frequency of each spectrum also shifts to lower frequencies for increasing P_{rf}, as predicted by Eq. (4) and the definition of κ in terms of ω_c. After calibrating the gain of the amplifier, we extract e_n^2 for each spectrum from a fit to the model of Fig. 1(c). The absolute effective temperature is then given by Eq. (6).

Equations (5) and (6) predict that the cantilever's effective temperature should fall with increasing P_{rf}, as demonstrated by the data in Fig. 3 for low power. With no rf applied we find $T_{eff} = 310(20)$ K. The coldest spectrum corresponds to a temperature of 45(2) K, a factor of 6.9 reduction. The minimum temperature appears to be limited by AM noise from our rf source. This noise power at $\Omega_{rf} \pm \omega_c$ is constant relative to the carrier, leading to a noise power at ω_c given by $e_n(\text{rf})^2 \propto P_{rf}^2$. We fit the residual noise $e_n(\text{rf})^2$ to a quadratic in P_{rf}, giving the dashed line temperature prediction in Fig. 3. From this fit we determine that the AM noise of our source is −170 dBc/Hz, reasonably consistent with the value (−167 dBc/Hz) measured by spectrum analysis.

The inset shows the cantilever damping rate Γ versus P_{rf}. The slope is $\Gamma'/P_{rf} = 5450(70)$ Hz/W, slightly higher than the value 3970 Hz/W calculated from Eq. (5) and the nominal cantilever dimensions. The nonlinearity in Γ'/P_{rf} at higher powers is consistent with the cantilever being pulled toward the rf electrode. We have numerically simulated this effect and find reasonable agreement. The variation of κ with P_{rf} (not shown) is also linear, with a slope $\kappa/P_{rf} = 7.64(8)$ W^{-1}, compared with the value 3.45 W^{-1} calculated from Eq. (4).

Although Γ'/P_{rf} and κ/P_{rf} differ from their predicted values, this disagreement is not unexpected considering the relatively large variations in dimensions d_0 and s [27]. Another indication of these uncertainties is that optical measurements of the static deflection of the cantilever along its length disagree with predictions based on a constant cantilever cross section. This will lead to deviations from our calculated values of ξ', ξ'', and ξ_c''. However, we stress that these deviations should not give significant errors in our measured values of L_{eq}, R_{eq}, and therefore our determination of T_{eff}.

To further test the model, we examine Γ and ω_c as a function of $\Delta\Omega$ (Fig. 4). For large detunings $\Delta\Omega$, Γ asymptotically approaches the value obtained in Fig. 3 for $P_{rf} = 0$. Near $\Delta\Omega = 0$, f_c is generally shifted to a lower value, while Γ is either enhanced or suppressed,

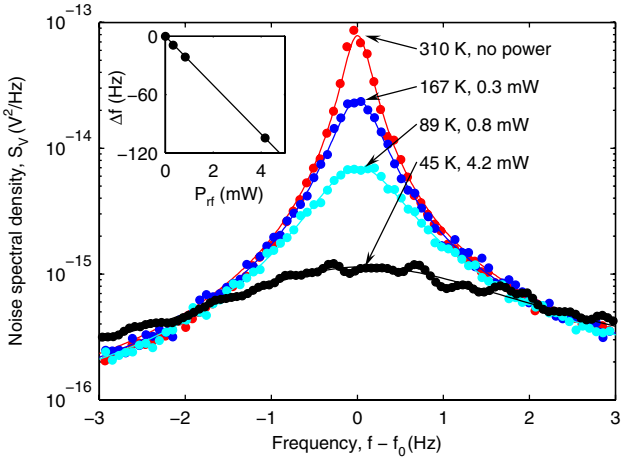

FIG. 2 (color online). Cantilever thermal spectra for four values of rf power. The x axis for each spectrum has been shifted to align the maxima of the three data sets. S_v is the measured noise referred to the input of the amplifier. Solid lines are fits to the model in Fig. 1(c), giving the temperatures indicated by arrows. (Inset) Cantilever frequency shift Δf vs rf power.

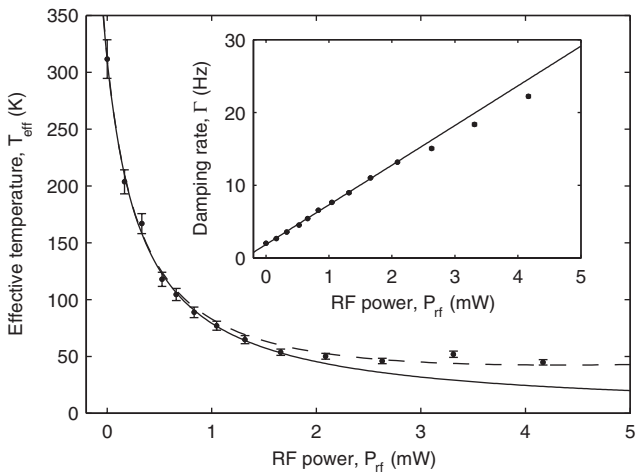

FIG. 3. T_{eff} as a function of rf power. The solid line is the temperature predicted by Eq. (6) using Γ from the fit in the inset and $e_n = e_n(R_{eq})$, while the dashed line takes into account additional noise due to the rf source. (Inset) Damping rate vs rf power. The solid line is a linear fit to the first ten points.

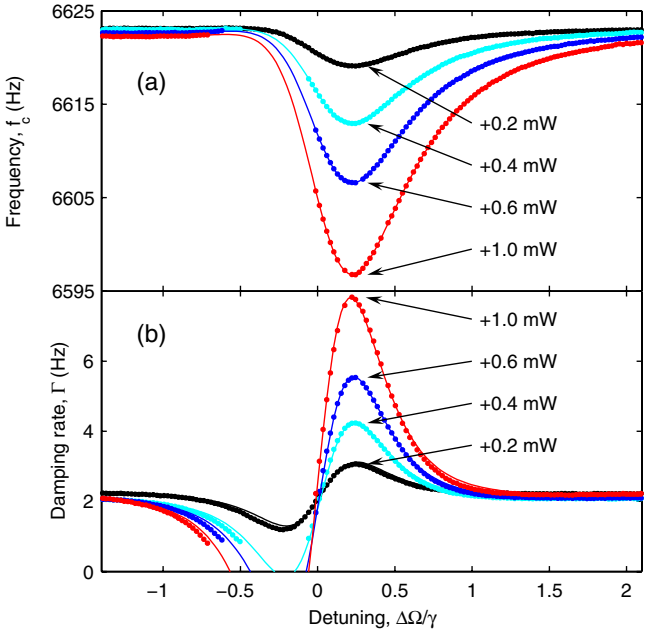

FIG. 4 (color online). Variation of the cantilever resonance with respect to rf frequency. (a) Cantilever frequency f_c and (b) damping rate Γ vs normalized rf detuning $\Delta\Omega/\gamma$ for several values of P_{rf}. The missing points between -0.7 MHz and 0 MHz correspond to a region of instability where Γ becomes negative. Solid lines are fits to Eqs. (4) and (5).

according to the sign of $\Delta\Omega$. Data cannot be obtained for $\Delta\Omega < 0$ when the rf power level is sufficient to drive the cantilever into instability ($\Gamma < 0$). The solid line fits show good agreement with the predicted behavior. From these fits we extract $C_c = 0.09$ pF, lower than the value 0.17 pF obtained from the physical dimensions. This disagreement is not surprising for the reasons mentioned above.

Some experiments using optical forces have observed strong effects from the laser power absorbed in the cantilever mirror. A conservative estimate of the rf power dissipated in our cantilever gives a temperature rise of less than 1 K at the highest power, so these effects should not be significant.

Although rather modest cooling is obtained here, the basic method could eventually provide ground state cooling. For this we must achieve the resolved sideband limit, where $\omega_c > \gamma$ [25,28], and the cooling would be very similar to the atomic case [3,4]. To insure a mean quantum number n less than one, the heating rate from the ground state $\dot{n}_{\mathrm{heat}} = \Gamma k_B T_c/(\hbar\omega_c)$ must be less than the cooling rate for $n = 1 \rightarrow 0$. The cooling rate $\dot{n}_{\mathrm{cool}}$ can be estimated by noting that each absorbed photon on the lower sideband (at the applied rf frequency $\Omega_0 - \omega_c$) is accompanied by reradiation on the rf "carrier" at Ω_0. If we assume the lower sideband is saturated for $n \approx 1$, $\dot{n}_{\mathrm{cool}} \approx \gamma/2$. Hence we require $R \equiv \dot{n}_{\mathrm{heat}}/\dot{n}_{\mathrm{cool}} \approx 2k_B T_c Q_{\mathrm{rf}}/(\hbar\Omega_0 Q_c) \ll 1$. For example, if $T_c = 0.1$ K, $\Omega_0/(2\pi) = 20$ GHz, $Q_{\mathrm{rf}} = 5000$ (e.g., a stripline), and $Q_c = 20\,000$ we have $R \approx 0.05$. For resolved sidebands, we require $\omega_c/(2\pi) > 4$ MHz.

We thank S. Voran for the use of his lab space. We thank D. Howe, C. Nelson, and A. Hati for providing us with low-noise rf sources and for discussion, and we thank R. Simmonds and J. Bollinger for comments. This Letter, a submission of NIST, is not subject to US copyright.

*krbrown@boulder.nist.gov
†Present address: Los Alamos National Laboratory, MS D454, P-21, Los Alamos, NM 87545, USA.

[1] V. B. Braginskiĭ, A. B. Manukin, and M. Yu. Tikhonov, Sov. Phys. JETP **31**, 829 (1970).
[2] V. B. Braginsky and A. B. Manukin, *Measurement of Weak Forces in Physics Experiments* (The University of Chicago Press, Chicago, 1977).
[3] F. Diedrich, J. C. Bergquist, W. M. Itano, and D. J. Wineland, Phys. Rev. Lett. **62**, 403 (1989).
[4] C. Monroe *et al.*, Phys. Rev. Lett. **75**, 4011 (1995).
[5] D. M. Meekhof *et al.*, Phys. Rev. Lett. **76**, 1796 (1996).
[6] C. Monroe, D. M. Meekhof, B. E. King, and D. J. Wineland, Science **272**, 1131 (1996).
[7] A. Ben-Kish *et al.*, Phys. Rev. Lett. **90**, 037902 (2003).
[8] K. C. Schwab and M. L. Roukes, Phys. Today **58**, No. 7, 36 (2005).
[9] A. Naik *et al.*, Nature (London) **443**, 193 (2006).
[10] P.-F. Cohadon, A. Heidmann, and M. Pinard, Phys. Rev. Lett. **83**, 3174 (1999).
[11] O. Arcizet *et al.*, Phys. Rev. Lett. **97**, 133601 (2006).
[12] D. M. Weld and A. Kapitulnik, Appl. Phys. Lett. **89**, 164102 (2006).
[13] D. Kleckner and D. Bouwmeester, Nature (London) **444**, 75 (2006).
[14] M. Poggio, C. L. Degen, H. J. Mamin, and D. Rugar, Phys. Rev. Lett. **99**, 017201 (2007).
[15] C. Höhberger Metzger and K. Karrai, Nature (London) **432**, 1002 (2004).
[16] J. G. E. Harris, B. M. Zwickl, and A. M. Jayich, Rev. Sci. Instrum. **78**, 013107 (2007).
[17] O. Arcizet *et al.*, Nature (London) **444**, 71 (2006).
[18] S. Gigan *et al.*, Nature (London) **444**, 67 (2006).
[19] T. Corbitt *et al.*, Phys. Rev. Lett. **98**, 150802 (2007).
[20] A. Schliesser *et al.*, Phys. Rev. Lett. **97**, 243905 (2006).
[21] J. M. W. Milatz, J. J. Van Zolingen, and B. B. Van Iperen, Physica (Amsterdam) **19**, 195 (1953).
[22] D. J. Wineland *et al.*, arXiv:quant-ph/0606180.
[23] H.-J. Butt and M. Jaschke, Nanotechnology **6**, 1 (1995).
[24] This expression for d neglects the curvature of the flexural mode and is strictly true only for $h \ll h_c$ and $d_0 \ll w, h$.
[25] F. Marquardt, J. P. Chen, A. A. Clerk, and S. M. Girvin, Phys. Rev. Lett. **99**, 093902 (2007).
[26] D. J. Wineland and H. G. Dehmelt, J. Appl. Phys. **46**, 919 (1975).
[27] The uncertainties for these numbers are a few micrometers, stemming from spatial nonuniformity in our etch process.
[28] I. Wilson-Rae, N. Nooshi, W. Zwerger, and T. J. Kippenberg, Phys. Rev. Lett. **99**, 093901 (2007).